

Measurement Methods for Flux Residue Quantity after Controlled Atmosphere Brazing of Aluminum Coolers

Śławomir NADOLNY¹, Adam HAMROL¹, Michał ROGALEWICZ¹, Adam PIASECKI²

¹ Poznan University of Technology, Faculty of Mechanical Engineering, Poland

² Poznan University of Technology, Faculty of Materials Engineering and Technical Physics, Poland

Received: 25 May 2023

Accepted: 28 August 2023

Abstract

The Controlled Atmosphere Brazing (CAB) process together with NOCOLOK[®] flux is associated with the occurrence of potassium fluoroaluminate residue inside the cooler. Excess of this flux residue is known to cause gelation of the coolant, which deteriorates the efficiency of the cooler. The flux residue amount is most often measured via Atomic Absorption Spectroscopy (AAS), in accordance with DIN ISO 9964-3. This is a time-consuming measurement that requires the use of specialized equipment and costly solvents. The following article presents two innovative methods for flux residue measurement after CAB process. They include Scanning Electron Microscopy (SEM) with Energy-Dispersive X-ray Spectroscopy (EDS) and Reflected Light Microscopy (RLM) with Differential Interference Contrast (DIC) module. The accuracy of these methods has been compared to the reference AAS method to evaluate their potential as alternative, less expensive, and quicker measurement methods for determining the quantity of flux residue.

Keywords

Heat Exchangers; Brazing; NOCOLOK; Paint-Flux; Potassium Fluoroaluminate; Metallography.

Introduction

At MAHLE Behr Ostrów Wielkopolski, air coolers manufacturing company, research is being conducted on the Controlled Atmosphere Brazing (CAB) process using NOCOLOK[®] flux. The aim of these studies is to minimize flux residue while ensuring the integrity of the air cooler. The CAB process is the most commonly used brazing technology in the automotive industry, especially for complex geometry connections (Gao et al., 2022). It enables continuous production with relatively low costs. The CAB process is carried out in a tightly controlled atmosphere, usually nitrogen, where the O₂ content does not exceed 40 ppm. This is done in a tunnel furnace that is divided into zones, corresponding to the sequential stages of the process: surface cleaning, material heat-

ing, filler metal melting, liquid filler metal flow, mutual diffusion phase, cooling, and solidification of the brazed joint (Zhao & Woods, 2013). The convective-radiative interaction allows the brazing of enclosed structures, including thin-walled joints. To facilitate the formation of brazed joints in hard-to-reach areas, an aluminum alloy with an Al-Si filler metal coating is utilized, the specific type of which depends on the requirements of the final product (Mirski & Pabian, 2017). The brazed joint is formed due to the difference in diffusion rates between Si and Al elements, resulting from the Kirkendall effect (Wu et al., 2021).

A challenge in the CAB process is the amorphous layer of aluminum oxide that forms immediately upon the contact of the aluminum alloy with oxygen (Wu et al., 2019). It hinders the wetting of the filler metal, preventing proper capillary action, required to fill the gaps between the joined materials. As a result, the aluminum oxide layer disrupts the diffusion process with the base material (Klett et al., 2022). Therefore, it is necessary to remove this layer before brazing. This is achieved by using an inorganic salt called flux. The surface of the base material has microscopic porosity, resulting from the difference in thermal expansion. The flux, when reaching its liquidus temperature, exhibits low surface tension. This allows it to

Corresponding author: Śławomir Nadolny – Poznan University of Technology, Faculty of Mechanical Engineering; MAHLE Behr Ostrów Wielkopolski, ul. Wodna 15; 63-400 Ostrów Wielkopolski, Poland, phone: +48 62 59 50 286, e-mail: slawomir.nadolny@doctorate.put.poznan.pl

© 2023 The Author(s). This is an open access article under the CC BY license (<http://creativecommons.org/licenses/by/4.0/>)

penetrate microchannels under the aluminum oxide layer, reaching the non-uniform layer of the base material. As a result, the aluminum oxide is lifted, dispersed, and ultimately dissolved (Kneba, 2006).

In the automotive industry, NOCOLOK® flux is the most commonly used flux (Gao et al., 2022). It is a non-hygroscopic, white powder, with a defined particle size distribution, based on the eutectic mixture of potassium fluoroaluminate KAlF_4 - K_3AlF_6 . Due to its low solubility in water (1.5–4.5 g/l), it is non-corrosive (NOCOLOK Encyclopedia, 2013). The flux is sensitive to the presence of magnesium in an aluminum alloy. It disrupts its effectiveness (Hawskworth, 2013). This is manifested by the formation of MgAl_2O_4 and K_2MgF_4 compounds, resulting in reduced flux fluidity (The Morphology and Structure of Post-Braze Flux Residues, 2011). To counteract this phenomenon, the flux is enriched with a maximum of 2% addition of cesium that interacts with magnesium, forming CsMgF_3 and $\text{Cs}_4\text{Mg}_3\text{F}_{10}$ compounds. Excess flux after the CAB process remains inside the cooler as flux residue. The flux residue appears as square-shaped plates measuring 10–20 μm , consisting of potassium fluoroaluminate, as well as needle-like shapes, composed of magnesium fluorides (NOCOLOK® Aluminium brazing webinar, 2021). The exact structure of the flux residue depends primarily on the flux weight on the components and the content of supporting elements (e.g., cesium, lithium). The parameters of the brazing process are also important, such as brazing temperature and time, furnace atmosphere (oxygen content), and humidity (affecting the dew point) (Gao et al., 2022).

Undesirable interactions between flux residue and the coolant liquid are known. This is manifested by the leaching of flux residue particles from inside the cooler that in reaction with additives in the coolant composition leads to gelation. This phenomenon reduces the homogeneity of the coolant and adversely affects heat conductivity (Mirski & Pabian, 2017). Additionally, accumulated solid particles of flux residue can detach from the inner surface of the cooler, causing clogging or blockage of narrower passages (Wojdat et al., 2019). This negatively affects the cooling system and can lead to vehicle overheating. Therefore, in the CAB process, careful control of flux application on components is required. The recommended flux weight for NOCOLOK® flux, as advised by the manufacturer, is 3–5 g/m² (NOCOLOK Encyclopedia, 2013).

In the automotive industry, the accepted method for measuring flux residue quantity is Atomic Absorption Spectrometry (AAS) in accordance with DIN ISO 9964-3 standard “Determination of sodium and potassium by flame emission spectrometry.” The AAS

method utilizes the emission of spectral lines by atoms excited in a burner flame. Subsequently, by utilizing the phenomenon of electromagnetic radiation absorption, characteristic to each element, the concentration of elements in the tested sample can be measured. There is no known analytical measurement line for fluorine (Ritgen, 2023). Nevertheless, the element potassium has measurement lines, with the most sensitive wavelength being 766.491 nm (Welz, 2005). This property is used to measure the flux residue quantity in the cooler, after the CAB process.

In the AAS method, the test sample is a solution of formic acid that circulates within the closed system of the cooler, dissolving flux residue particles. Therefore, the tested cooler must be hermetic. Next, the formic acid from the sample solution is evaporated using an atomizer, and atomic vapor is generated using a nebulizer. It is then irradiated by a hollow cathode lamp, selected for the potassium wavelength, allowing for ionization (Ritgen, 2023). The discharge of potassium ions on the cathode of the lamp emits electromagnetic radiation. The intensity of this radiation is recorded by the spectrometer detector and converted into potassium element concentrations, expressed as [mg/cooler]. This method is characterized by high sensitivity to the presence of potassium in quantities as low as 1.2 pg (Welz, 2005). However, it requires the use of specialized research equipment. The AAS method is a destructive examination that uses significant amounts of solvent. It is associated with high costs and time-consuming measurements. Therefore, in the production process, the control of flux residue in coolers is performed periodically, according to individually determined requirements for each product.

Finding a measurement method that allows for fast, cost-effective, and reliable measurement of flux residue quantity in the cooler after the CAB process is a challenge, which has been undertaken as part of the research work conducted at MAHLE Behr Ostrów Wielkopolski. Based on knowledge and experience in the production of air coolers, alternative measurement methods that enable the determination of flux residue quantity have been considered. These methods are based on commonly used techniques in companies implementing the CAB process. They include Scanning Electron Microscopy (SEM) and Reflected Light Microscopy (RLM). The phenomena of excited electron radiation and the surface area of flux residue particles observed on the air cooler samples have been examined. The potential of these methods, as reliable means of measuring flux residue quantity after the CAB process, has been compared with the reference AAS method.

Alternative methods for measuring flux residue quantity

Scanning Electron Microscopy (SEM)

The application of SEM, combined with Energy-Dispersive X-ray Spectroscopy (EDS), allows for the measurement of element concentrations on the observed surface. This is achieved by using an electron beam that increases the energy of electrons and their ability to penetrate the sample, proportionally to the applied accelerating voltage. The emitted electrons, upon contact with atoms in the sample, excite them and emit characteristic X-ray radiation for specific elements (Rusanovsky et al., 2022). The EDS detector records this radiation and its intensity. Based on this, the proportional concentration of a specific element in the sample can be determined, providing results in weight percentage [wt%]. The measurement takes place inside the microscope chamber, under vacuum conditions.

The SEM-EDS method is commonly used in air cooler production for cleanliness control. It is typically used to examine the microstructure of aluminum alloys after the CAB process (The Morphology and Structure of Post-Braze Flux Residues, 2011) and the presence of contaminants inside the cooler (Lacaze, 2005). According to the knowledge of the author, there is currently no literature describing the application of SEM-EDS for measuring flux residue quantity after the CAB process.

To determine the flux residue quantity inside the cooler via the SEM-EDS method, it is necessary to identify the areas where the flux residue agglomerates. The concentration results of fluorine and potassium elements on the sample surface need to be summed, due to the presence of flux residue in two forms, KAlF_4 or K_3AlF_6 . Then, the obtained concentration of both elements needs to be averaged across the samples, in order to relate them to the entire cooler. SEM-EDS measurement is a destructive method. Due to the size limitations of the chamber, sample preparation of the appropriate size is necessary.

Reflected Light Microscopy (RLM)

The use of RLM allows for the direct observation of the surface of the cooler immediately after the CAB process. The identification of particles observed on the surface is based on the knowledge of the observer in regards of the composition of the used alloy and the expected inclusions on the surface. Therefore, prior examination (at least once) for each cooler type such as SEM-EDS is required to interpret the

images obtained through RLM observation. This enables a more accurate understanding of the expected topology of the samples and the composition of the particles present on them.

Observation using RLM typically requires the preparation of a metallographic sample, involving grinding, chemical etching, and embedding in resin (Rusanovsky, 2022). However, flux residue crystals occur only on the surface as transparent agglomerates that are susceptible to chemical factors. As a result, sample grinding, resin embedding, or chemical etching cannot be performed. These obstacles can be overcome by using the Differential Interference Contrast (DIC) module. DIC is applied to minimize distortions and can be used for topographical differences on the sample surface no smaller than $0.2\ \mu\text{m}$ (Aluminium Brazing News, 2011), while the flux residue has a thickness of $1\text{--}2\ \mu\text{m}$ (Shribak, 2006). The DIC module operates based on interferometry principles. It is used to enhance the contrast of unstained, transparent particles, which flux residue crystals can be classified as. The image is created by separating the light into two mutually polarized beams that illuminate the sample surface and then recombine before observation. As a result, an image that reproduces the edge lines of transparent particles present on the examined surface is formed (Scott and Schwab, 2019).

RLM observation is commonly used for the brazed joint inspection after the CAB process (Frøseth et al., 2003). However, the use of the RLM-DIC method for measuring the flux residue quantity after the CAB process is an innovative approach that according to the knowledge of the author has not been described in the literature.

To apply the RLM-DIC method, it is necessary to identify the areas where the flux residue agglomerates. The observed particle surface needs to be summed and then averaged across the samples in order to relate it to the entire surface of the cooler. RLM-DIC measurement is a destructive method, requiring the preparation of samples, adapted to the size of the microscope stage.

Testing of the flux residue quantity measurement methods: SEM-EDS and RLM-DIC

Methodology

The testing of alternative methods SEM-EDS and RLM-DIC was carried out on a standard charged air cooler (Fig. 1).

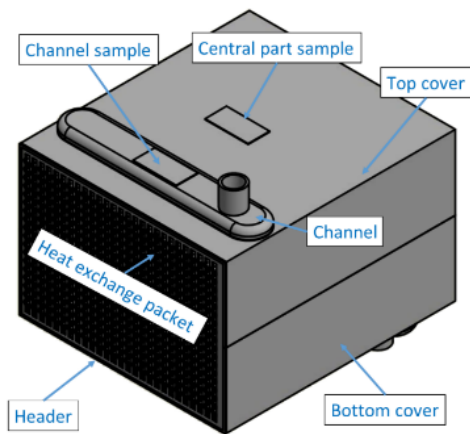


Fig. 1. 3D model of the charged air cooler (Source: Author own conception based on Autodesk Inventor Professional 2019 software)

This cooler has a hexagonal shape and consists of a heat exchange package enclosed by two headers and two U-shaped covers. The components of the cooler are made of EN AW-3003 aluminum alloy, clad on one side with an Al-Si filler metal layer. They undergo processes of pressing and rolling, followed by weighing. They are then spray-coated with a paint-flux, which is a mixture containing NOCOLOK[®] flux, binder, organic components, and traces of cesium, and weighed again. The obtained mass of flux is related to the surface area of the components, calculated based on the 3D model of the cooler, determining the coating weight. The headers, before the CAB process, are coated with the required flux weight ranging from 3–5 g/m², as specified by the manufacturer. The covers are coated with flux weighing between 0–7.5 g/m². These prepared coolers undergo the CAB process in a tunnel furnace, after which the flux residue quantity inside them is measured.

The results of measuring the flux residue quantity in the tested SEM–EDS and RLM–DIC methods depend on the sampling location. For this reason, four representative areas were selected in the cooler. The gravitational interaction on the flux after its transition into a liquidus state is expected to have a different impact. This is investigated through the symmetric division of the cooler into the top and bottom covers. The sampling locations are symmetrical on both top and bottom covers. The difference in the geometry of the cooler is also taken into account. The central part of the cover is in direct contact with the heat exchange package and requires the formation of a brazed joint at the connection between the components. On the other hand, the channel of the cover is an indentation and is not in contact with other

components. Therefore, a local temperature difference between them is expected after reaching the brazing temperature in the furnace, which can affect the quantity and shape of the flux residue. Taking this division into account, samples were cut out from the coolers in the shape of rectangles with dimensions of approximately 30 × 15 mm.

To enable a comparison between the SEM–EDS and RLM–DIC methods, four coolers with two levels of flux on the covers were prepared: 0 g/m² and 7.5 g/m². They were measured using the reference AAS method. The tested methods have different measurement specifications (Table 1).

Table 1
Comparison of flux residue quantity measurement methods (Source: Author own conception)

Measurement method	AAS	SEM–EDS	RLM–DIC
Measured physical quantity	Absorbance	X-ray radiation energy	Surface area of flux residue particles
Method of value determination	Spectrometer	EDS detector	Image processing
Measurement subject	Solution of solvent with flux residue	Surface of the sample	Surface of the sample

SEM–EDS method

The SEM–EDS observation of the samples was conducted using a Tescan Mira 3rd-generation microscope. The accelerating voltage of 12 kV was applied. This allowed for the determination of element concentrations along with electron images, where colors corresponded to specific elements. Intensely colored pixels indicated increased concentrations of a particular element, while darker areas indicated reduced presence or absence of that element. A limitation of this measurement is the inability to directly differentiate observed chemical compounds. Images of a 1 mm² area were captured at a magnification of ×200 for the tested samples.

Flux residue can be observed in the form of crystal agglomerates, as shown in magnifications of ×200 and ×1000 (Fig. 2). On image a) the expected coexistence of fluorine and potassium can be observed as easily distinguishable hexagonal crystals with an area of approximately ~ 30 μm², as well as rectangular shapes of an undefined size. Additionally, observable small crystals with the area below 1 μm² may indicate the presence of O₂ molecules above 40 ppm

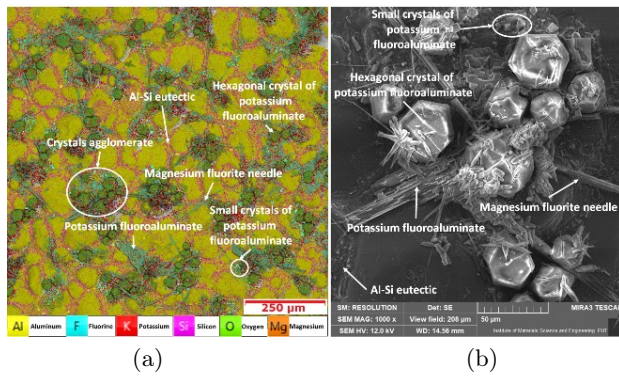


Fig. 2. SEM-EDS images of the sample after the CAB process: a) Magnification $\times 200$; b) Magnification $\times 1000$ of the crystals agglomerate (Source: PUT Faculty of Materials Engineering and Technical Physics)

inside the cooler. Which, according to the data provided by the manufacturer, is associated with the formation of hexagonal plates below $5 \mu\text{m}$ in size (NO-COLOK® Aluminium brazing webinar, 2021). On the other hand, image b) shows an agglomerate of flux residue crystals with a surface area of approximately $\sim 180 \mu\text{m}^2$, containing hexagonal crystals of potassium fluoroaluminate, with an average surface area of $29 \mu\text{m}^2$, as well as needles of magnesium fluoride MgF_2 with a thickness of $0.18\text{--}5.5 \mu\text{m}$.

For the analyzed sample, SEM-EDS images were also created with highlighted only selected elements (Fig. 3). The presence of magnesium fluoride needles indicates the occurrence of magnesium needling that in excess can create stress concentrations in brazed joints, leading to their cracking (Li & Arnborg, 2003). Significant clusters of cesium that could form as CsMgF_3 or $\text{Cs}_4\text{Mg}_3\text{F}_{10}$ crystals were not observed on the surface. It is also worth noting the accumulation of oxygen in the form of hexagonal crystals. This suggests that due to the closed structure of the cooler, oxygen from the dissolved aluminum oxide layer can interact with the flux residue, influencing crystal growth. The presence of silicon in areas devoid of fluorine, potassium, and oxygen can also be observed. For each sample obtained from 3 coolers, 5 images were taken at a magnification of $\times 200$. The elements considered were potassium and fluorine, as components of the flux residue. The obtained values of the total concentration of flux residue [wt%] were averaged and divided by the sampling locations. The relationship between the average concentration of fluorine and potassium to the flux weight on the covers is linear (Fig. 4).

There is also an increased flux residue quantity on the samples taken from the channel of the cover. This

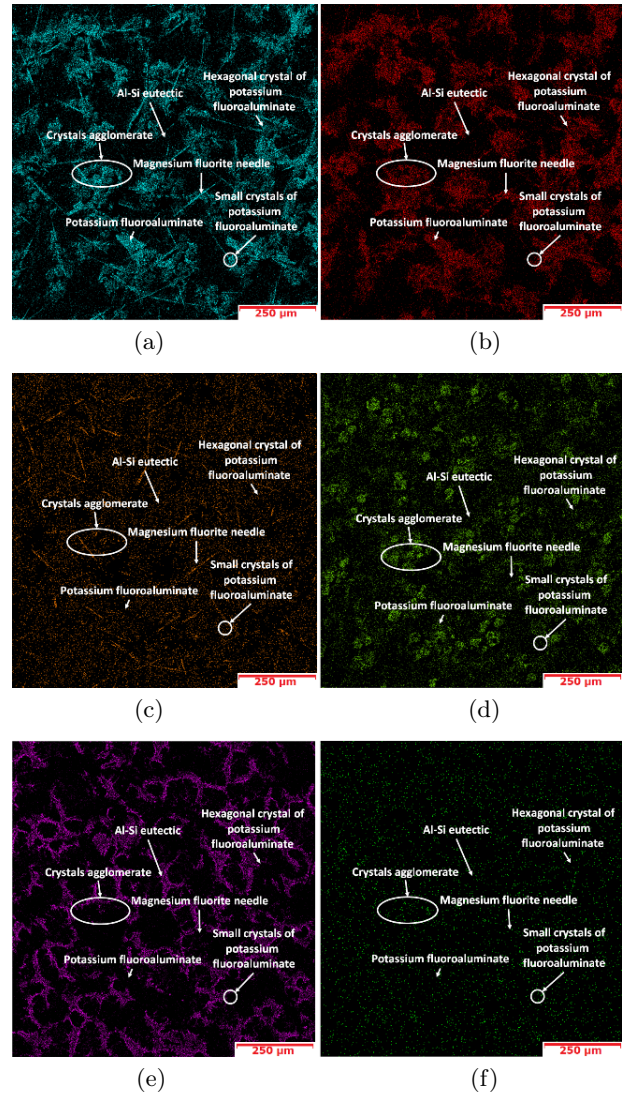


Fig. 3. SEM-EDS images of selected elements: a) Fluorine; b) Potassium; c) Magnesium; d) Oxygen; e) Silicon; f) Cesium (Source: PUT Faculty of Materials Engineering and Technical Physics)

is in line with the expectations since the flux present in the channel does not come into contact with other surfaces and therefore does not participate in the brazed joint formation. The differences in the flux residue quantity on the top and bottom covers do not change significantly within the flux weight range specified by the manufacturer ($3\text{--}5 \text{g/m}^2$). However, an excess of flux (above 6g/m^2) no longer actively participates in the brazed joint formation and is subject to the force of gravity. This results in the migration of flux residue from the top cover to the bottom cover. The obtained data demonstrates that the SEM-EDS method allows for determining the flux residue quantity inside the cooler after the CAB process.

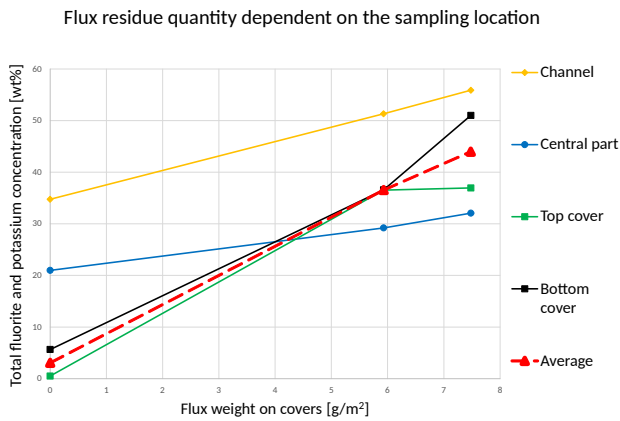


Fig. 4. Comparison of the SEM–EDS measurement results of the fluorine and potassium concentrations dependent on the sampling location (Source: Author own calculation)

RLM–DIC method

The observations of the same sample, with a flux weight of approximately 5 g/m² before the CAB process, using a) the SEM–EDS method and b) the RLM–DIC method can be compared (Fig. 5).

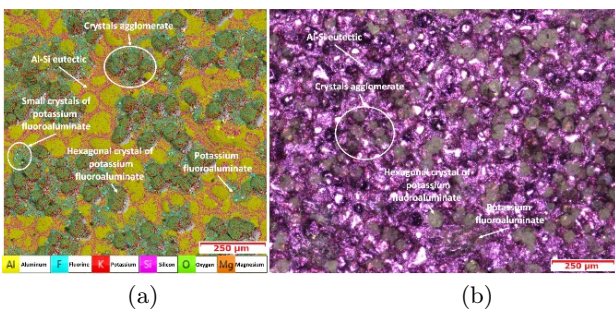


Fig. 5. Comparison of images: a) SEM–EDS b) RLM–DIC (Source: PUT Faculty of Materials Engineering and Technical Physics; Author own research)

In the SEM–EDS image of the 1 mm² area, 96 hexagonal shapes ranging in size 17–84 µm² are identified, with an average size of 46 µm². On the sharpened RLM–DIC image of area 1.5 mm², distinct potassium fluoroaluminate crystals are visible as yellow discoloration. It is possible to distinguish 151 hexagonal crystals ranging in size from 19–90 µm², with an average size of 50 µm². The eutectic Al–Si (magenta color) is visible between these particles, and it is discernible in both images. However, small potassium fluoroaluminate crystals (< 1 µm²) are difficult to identify on the RLM–DIC image. The results are consistent and allow for the interpretation of yellow discolorations as flux residue.

Image obtained using the RLM–DIC method requires graphical processing (Fig. 6a). To count the

flux residue quantity, the first step is to increase the yellow color balance. This further highlights the flux residue against the Al–Si background of the sample (Fig. 6b). This manipulation allows for reducing the intensity of colors (hue) while increasing their saturation (chrominance) while maintaining the contrast difference between flux residue particles. Next, to eliminate black and white reflections resulting from sample roughness, the colors of the image are inverted (Fig. 6c). The final step involves nullifying the brightness and combined saturation for the red, magenta, blue, cyan, and yellow colors while maximizing these parameters for the green color. The result of the graphic processing of the image is the flux residue that appears as a visible green color (Fig. 6d) Its content can be counted using a color histogram, as a percentage of green to color on the whole image. Considering the scale of the image, the percentile can be converted to area [mm²].

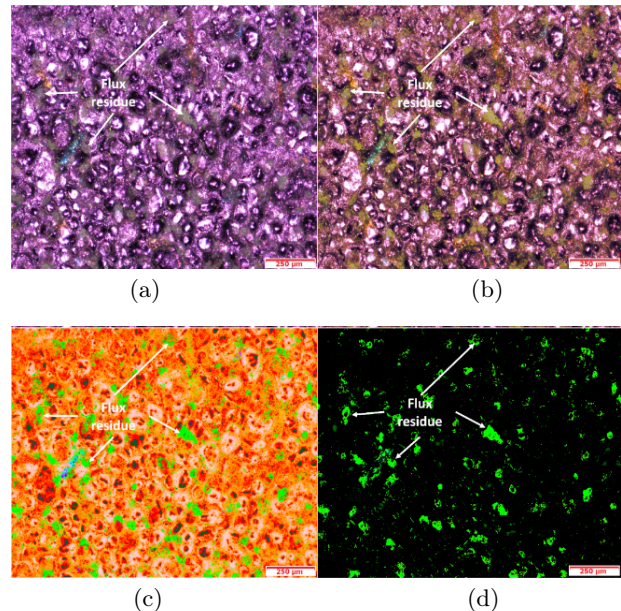


Fig. 6. Graphic processing of RLM–DIC images (Source: Author own conception based on Gimp 2.10 graphic software)

A total of 140 images were taken for 28 samples from 7 coolers, and the results were compared regarding differences arising from the sampling locations. A proportional increase in the average surface area of flux residue can be observed with an increase in the flux weight on the covers (Fig. 7). It was noted that the recorded surface area of flux residue is similar, regardless of the sampling location up to a flux weight threshold of ~ 6 g/m². Above this weight, the gravitational influence on the flux residue can be observed,

resulting in its migration from the top cover to the bottom cover.

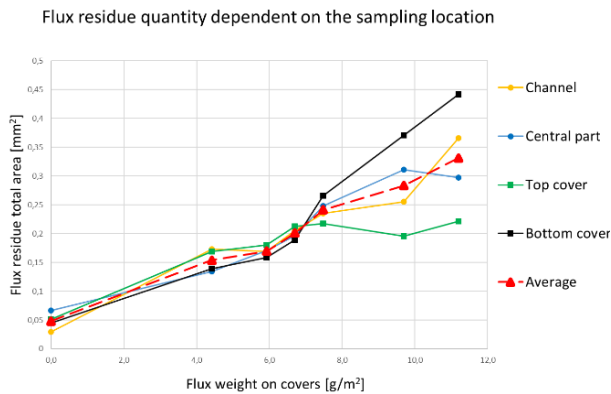


Fig. 7. Comparison of the RLM–DIC measurement results of the flux residue surface area dependent on the sampling location (Source: Author own calculation)

Results

The results of flux residue quantity measurements using SEM–EDS and RLM–DIC methods were compared with the reference method AAS (Table 2).

The normalized values obtained from these methods were compared (Fig. 8). For the SEM–EDS method, within the flux weight range of 0–7.5 g/m² on the covers before the CAB process, the relative error δ does not exceed 2.99%, compared to the reference AAS method. The coefficient of determination for the fitted trendline is $R^2 = 0.9978$, indicating a direct proportionality of the obtained results. For the RLM–DIC method, the relative error δ does not ex-

Table 2

Summary of the results of flux residue quantity measurement methods (Source: Author own calculation)

Measurement method	Recorded data				
	0	4.42	5.93	6.71	7.48
Flux weight on covers [g/m ²]	0	4.42	5.93	6.71	7.48
AAS Method* Normalized Value	0	–			1
SEM–EDS Method [wt%]	3.06	–	37.35	–	43.96
SEM–EDS Method Normalized Value	0	–	0.84	–	1
RLM–DIC Method [mm ²]	0.05	0.15	0.17	0.20	0.24
RLM–DIC Method Normalized Value	0	0.55	0.63	0.79	1

*AAS method data before normalization is covered by the trade secret

ceed 8.62% and the coefficient of determination for the fitted trendline is $R^2 = 0.9831$, also indicating a direct proportionality.

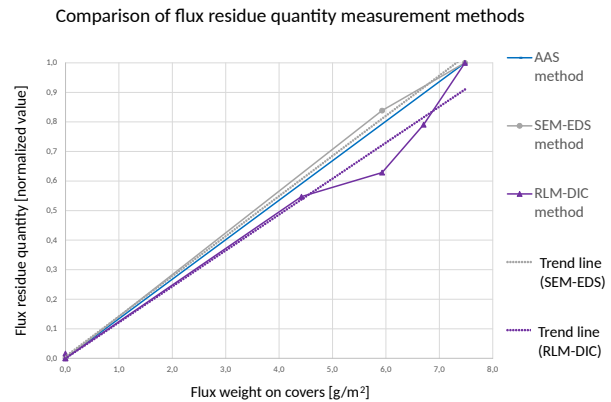


Fig. 8. Comparison of normalized values of flux residue quantity measurement methods results (Source: Author own calculation)

Conclusions

Compared to the reference AAS method, both SEM–EDS, and RLM–DIC methods are associated with lower measurement costs and are less time-consuming. In particular, the RLM–DIC method does not require specialized measuring apparatus or chemical reagents, resulting in the lowest cost. Additionally, both methods allow for separate measurements of selected areas of the cooler. This enables the identification of regions with excessive accumulation of flux residue, which can lead to corrosion risk (NOCOLOK Encyclopedia, 2013).

However, the disadvantage of both SEM–EDS and RLM–DIC is that they are destructive measurement methods. They require identification of these flux residue agglomeration regions and thereby selecting sampling locations for each type of the cooler. In order to relate the surface of the flux residue, or the concentration of fluorine and potassium elements, to the quantity of flux residue inside the entire cooler, a reference chart is needed. This chart must show the dependence of the input flux weight on the flux residue quantity after the CAB process. The values have to be obtained using the AAS method at least once for each given type of cooler.

Based on the obtained results, it can be concluded that both SEM–EDS and RLM–DIC methods can be effectively utilized in serial production for measuring flux residue quantity after the CAB process. The SEM–EDS method allows for results consistent with the reference AAS method but still require a spe-

cialized measuring apparatus and incurs significant costs. On the other hand, the RLM–DIC measurement method is characterized by lower accuracy, but sufficient precision. In exchange, it offers greater speed and low cost.

Acknowledgments

The research was conducted as a part of the Applied Doctorate Program of the Ministry of Education and Science implemented in the years 2021–2025 (Agreement No. DWD/(PP)RU00019673). The partner of the conducted research is MAHLE Behr Ostrów Wielkopolski Sp. z o.o.

References

- Aluminium Brazing News. (2011). Knowledge & Technology, Post-Braze Flux Residue Properties. www.aluminium-brazing.com/2011/03/16/post-braze-flux-residue-properties-2/. [Accessed: 09-May-2023]
- Frøseth, A.G., Høier, R., Derlet, P., Andersen, S., & Marioara C. (2003). Bonding in MgSi and Al-Mg-Si compounds relevant to Al-Mg-Si alloys. *Physical Review B*, 67(22), 224106. DOI: [10.1103/PhysRevB.67.224106](https://doi.org/10.1103/PhysRevB.67.224106).
- Gao, Z., Qin, Z., & Lu, Q. (2022). Controlled Atmosphere Brazing of 3003 Aluminum Alloy Using Low-Melting-Point Filler Metal Fabricated by Melt-Spinning Technology. *Materials*, 15(17), 6080, MDPI. DOI: [10.3390/ma15176080](https://doi.org/10.3390/ma15176080).
- Hawksworth, D.K., (2013). *Fluxless brazing of aluminium*. *Advances in brazing*, Woodhead publishing, 566–585. DOI: [10.1533/9780857096500.3.566](https://doi.org/10.1533/9780857096500.3.566).
- Klett, J., Bongratz, B., Viebranz, V. F., Kramer, D., Hao, C., Maier, H. J., & Hassel, T. (2022). Investigations into Flux-Free Plasma Brazing of Aluminum in a Local XHV-Atmosphere. *Materials*, 15(23). DOI: [10.3390/ma15238292](https://doi.org/10.3390/ma15238292).
- Kneba, Z. (2006). Model of a plate cooler working in the cooling system of a car internal combustion engine. *Automotive Archive* (in Polish), pp. 373–385.
- Lacaze, J., Tierce, S., Lafont, M-C., Thebault, Y., Pèbère, N., Mankowski, G., Blanc, C., Robidou, H., Vau-mousse, D., & Daloz, D. (2005). Study of the microstructure resulting from brazed aluminium materials used in heat exchangers. *Materials Science and Engineering: A*, 413, pp. 317–321. DOI: [10.1016/j.msea.2005.08.187](https://doi.org/10.1016/j.msea.2005.08.187).
- Li, Y.J., & Arnberg, L. (2003). Evolution of eutectic intermetallic particles in DC-cast AA3003 alloy during heating and homogenization. *Materials science and engineering: A*, 347(1–2), pp. 130–135. DOI: [10.1016/S1359-6454\(03\)00160-5](https://doi.org/10.1016/S1359-6454(03)00160-5).
- Mirski, Z., & Pabian, J. (2017). Modern trends in the production of brazed heat exchangers for the automotive industry. *Welding Review* (In Polish), 89.
- NOCOLOK® Aluminium brazing webinar. (2021). Solvay Fluor. www.aluminium-brazing.com/2021/02/04/nocolok-aluminium-brazing-webinar-successful-and-well-received. [Accessed: 12-Feb-2023]
- NOCOLOK Encyclopedia. (2013). Solvay Special Chemicals. www.aluminium-brazing.com/sponsor/nocolok/Files/PDFs/NOCOLOK-Encyclopedia-2013.pdf. [Accessed: 09-May-2023]
- Ritgen, U. (2023). *Atomic Absorption Spectroscopy (AAS)*. *Analytical Chemistry I*, Springer Berlin Heidelberg, pp. 247–253. DOI: [10.1007/978-3-662-66336-3_21](https://doi.org/10.1007/978-3-662-66336-3_21).
- Rusanovsky, M., Beeri, O., & Oren, G., (2022). An end-to-end computer vision methodology for quantitative metallography. *Scientific Reports*, 12(1), 4776. DOI: [10.1038/s41598-022-08651-w](https://doi.org/10.1038/s41598-022-08651-w).
- Scott, D.A., & Schwab, R. (2019). Principles and Practice of Metallography. *Metallography in Archaeology and Art*, 19–68. DOI: [10.1007/978-3-030-11265-3_3](https://doi.org/10.1007/978-3-030-11265-3_3).
- Shribak, M., & Inoué S. (2006). Orientation-independent differential interference contrast microscopy. *Applied Optics*, 45(3), 460–469. DOI: [10.1364/AO.45.000460](https://doi.org/10.1364/AO.45.000460).
- The Morphology and Structure of Post-Braze Flux Residues (2011). www.aluminium-brazing.com/sponsor/nocolok/Files/PDFs/Morphology_Paper.pdf. [Accessed: 09-May-2023]
- Welz, B., Helmut, B-R., Florek, S., & Heitmann, U. (2005). *High-resolution continuum source AAS: The better way to do atomic absorption spectrometry*. John Wiley & Sons. DOI: [10.1021/ja0597395](https://doi.org/10.1021/ja0597395).
- Wojdat, T., Winnicki, M., Mirski, Z., & Żuk, A. (2019). An innovative method of applying fluxes using the low-pressure cold gas spraying method. *Welding Technology Review*, 91(10), 17–24. DOI: [10.26628/wtr.v91i10.1052](https://doi.org/10.26628/wtr.v91i10.1052).
- Wu, G., & Dash, K. (2019). Oxidation studies of Al alloys: part II Al-Mg alloy. *Corrosion Science*, 155, 97–108. DOI: [10.1016/j.corsci.2019.04.018](https://doi.org/10.1016/j.corsci.2019.04.018).
- Wu, Y., Yu, CN., & Sekulic, D.P. (2021). Si diffusion across the liquid/solid interface of capillary driven (Al–Si)–K_xAl_yF_z micro-layers. *Journal of Materials Science*, 56, 7681–7697. DOI: [10.1007/s10853-020-05689-x](https://doi.org/10.1007/s10853-020-05689-x).
- Zhao, H., & Woods, R. (2013). *Controlled atmosphere brazing of aluminum*, in *Advances in brazing*, Woodhead Publishing, pp. 280–323e. DOI: [10.1533/9780857096500.2.280](https://doi.org/10.1533/9780857096500.2.280).